



HAL
open science

X-ray spectra of spontaneous emission in the bandgap of a 1D photonic crystal

Jean-Michel André, Philippe Jonnard

► **To cite this version:**

Jean-Michel André, Philippe Jonnard. X-ray spectra of spontaneous emission in the bandgap of a 1D photonic crystal. 2024. hal-04584648

HAL Id: hal-04584648

<https://hal.science/hal-04584648>

Preprint submitted on 23 May 2024

HAL is a multi-disciplinary open access archive for the deposit and dissemination of scientific research documents, whether they are published or not. The documents may come from teaching and research institutions in France or abroad, or from public or private research centers.

L'archive ouverte pluridisciplinaire **HAL**, est destinée au dépôt et à la diffusion de documents scientifiques de niveau recherche, publiés ou non, émanant des établissements d'enseignement et de recherche français ou étrangers, des laboratoires publics ou privés.



Distributed under a Creative Commons Attribution - NonCommercial 4.0 International License

X-ray spectra of spontaneous emission in the bandgap of a 1D photonic crystal

Jean-Michel André, Philippe Jonnard

Laboratoire de Chimie Physique—Matière et Rayonnement, Faculté des Sciences et Ingénierie, Sorbonne Université, UMR CNRS, 4 place Jussieu, 75252 Paris Cedex 05, France

Abstract

The alteration by Purcell effect of the spontaneous emission spectrum from within one-dimensional photonic band gap crystal is investigated in the x-ray domain. The Si $L_{2,3}$ emission band from a bulk specimen is recorded by means of an original spectroscopic instrument and regarded as a reference spectrum. A Mo/Si periodic multilayered structure forming a one-dimensional photonic crystal (1D-PC) is considered. The Si $L_{2,3}$ spectrum is calculated from the reference spectrum when the spontaneously emitted radiation is Bragg diffracted by the 1D-PC. It appears that the spectrum from the 1D-PC in the Bragg condition is considerably modified with respect to the reference spectrum with a strong inhibition of the emission within the band gap. The anomalous Lamb optical shift of the spontaneous emission from the 1D-PC is also estimated ; it is shown that this shift cannot be observed with a mere standard x-ray spectrometer.

Keywords

X-ray spectrum ; photonic crystal ; spontaneous emission

1. Introduction and context

Following Purcell's article published in 1946 (Purcell, 1946), the community involved in quantum electrodynamics (QED) became aware that the spontaneous emission (SE) of an atomic system depends on the boundary conditions imposed on the system. Thus, an atom placed in an “optical box” (cavity, photonic crystal, waveguide, etc.) may not emit as if it was placed in vacuum : emission may be inhibited or, on the contrary, exalted. This phenomenon is known as the Purcell effect. This pioneering work led to the development of a new field of QED : the cavity quantum electrodynamics (C-QED) (Haroche and Kleppner, 2008). This discipline was revived with the appearance of the photonic crystal (PC) concept introduced by E. Yablonovitch and T. J. Gmitter in 1989 (Yablonovitch and Gmitter, 1989). These optical devices, which can be of natural origin such as opals, or synthetic, are analogous to crystals in that they exhibit periodic modulation of their optical structure, *i.e.* generally of their dielectric constant. The C-QED, which had previously concentrated on optical cavities (high-quality cavities, Fabry-Pérot resonators, for example), has extended its range to the one of PC, creating what can be called P-QED and to the one of the waveguides leading to the W-QED emerging field (Sheremet et al., 2023).

An important subject that began to be addressed in this context at the end of the 20th century was the dynamics of spontaneous emission in bandgap regions (John and Quang, 1994; Nabiev et al., 1993; Vats et al., 2002) : non-Markovian decay processes have been demonstrated. Generally speaking, cavity, PC or waveguide form some kinds of traps for photons, which then undergo confinement where the interaction with atoms can be stronger than in a vacuum. This results in a number of phenomena :

- the non-Markovian interaction can be accompanied by photon-atom bound states with dressed atoms (John and Quang, 1995; John and Wang, 1991) resulting for the SE in damped Rabi oscillations ;
- quantum interference effects in the SE of atoms embedded in a PC have been demonstrated (Zhu et al., 1997) ;
- an anomalous Lamb optical shift (ALOS) has been predicted (John and Wang, 1990) then theorised with different forbidden bandgap models : gap with isotropic or anisotropic dispersion, pseudo-gap.

ALOS is the difference in energy (frequency) between that associated with an atomic transition occurring in an optical box and that occurring in a bulk material. This

change in energy levels is attributable to the modification of the coupling between the atom and the photons from the photonic reservoir that enables SE, given that the atom emits and re-absorbs so-called virtual photons (no conservation of energy during the process) under different conditions depending on whether it is in vacuum or in an optical box. The atom-photon interaction depends crucially on the structure of the photonic reservoir and, more precisely, on the density of photonic modes (DOM) : a vacuum has a DOM that varies monotonically with energy, whereas a cavity has a DOM that varies markedly in the resonance regions of single cavities or waveguides or in the band gaps of PC. Cooperative effects, such as superradiance occurring when initially excited atoms are confined in a volume with dimensions much smaller than the radiation wavelength, have also been reported (Lambropoulos et al., 2000).

Following the first demonstration in the microwave range (Yablonovitch et al., 1991) of the operation of a PC, experimental activity focused mainly on the visible and near-infrared ranges, with the aim of finding applications in telecommunications. It was not until several decades, after the first artificial structures were produced on the nanometric scale in the 1970s (Attwood, 1999), that work in C-QED was extended to the short wavelength range. This delay can be explained by the difficulty of producing PC on a (sub-)nanometer scale adapted to this spectral range, as well as by technological constraints in terms of radiation sources and detection. However, the extension of C-QED to the field of X-ray and X-UV radiations is highly desirable insofar as these spectral ranges include radiation that interacts strongly with the electrons in matter, which is an essential tool for solid-state physics and materials science.

In 1996, J.-P. Chauvineau et al. (Chauvineau et al., 1996; Chauvineau and Bridou, 1996) have succeeded in observing Kossel diffraction in the soft X-ray region for the K fluorescence of iron using a periodic multilayer, similar to a one-dimensional PC (1D-PC). Kossel diffraction refers to the diffraction in Bragg condition of radiation emitted spontaneously (fluorescent SE or characteristic emission) by an element located within the diffracting periodic structure ; it can be seen as the inverse process of the standing wave system in the sense that the location of the source and the observer are reversed (Gog et al., 1994). The work of Chauvineau et al. paved the way for a series of studies on Kossel diffraction generated by other means of excitation: electrons, synchrotron radiation and protons (Le Guen et al., 2019). Kossel diffraction can be seen as a facet of

the Purcell effect, as shown by experimental work carried out in the field of soft X-rays (André and Jonnard, 2010).

In this work, we continue to develop this point of view by analysing the X-ray spectra of the SE within a PC in the region of a band gap. The SE spectrum of an element, in this case the $L_{2,3}$ emission band ($3sd - 2p$ transition) of silicon, is measured in a bulk material and the SE spectrum of the same element (*i.e.* Si) in a 1D-PC forming a Bragg resonator is calculated in the band gap region corresponding to the first Bragg peak. The calculation is based on the spectrum obtained in the bulk structure using an approach proposed in various works (André and Jonnard, 2010; Dowling and Bowden, 1992) requiring the determination of the DOM and the normal modes (NM) of the PC.

SE spectra in PC have previously been observed in the visible range (Kuroda et al., 2009; Tocci et al., 1996) demonstrating an exaltation linked to the increase in the DOM at the bandgap edge. Q. Liu et al. (Liu et al., 2010) succeeded in demonstrating an ALOS in the visible range in a 3D-PC consisting of an inverse opal and carried out measurements of this in very good agreement with the model of N. Vats et al. (Vats et al., 2002). In the X-ray field, the work mainly concerned the W-QED: J. Haber et al. demonstrated a modification of the characteristic L_3 spectrum of tantalum in a film inserted in a cavity; they observed a collective optical Lamb shift accompanied by a superradiance and Fano resonance effect (Haber et al., 2019). Our study is part of this context, with the waveguide cavity replaced by a 1D-PC.

In this work, the SE dynamics in the band gap region of a 1D-PC will also be addressed. It is important to note that a 1D-PC has a full gap with isotropic dispersion unlike a 3D-PC, which generally has a pseudo-gap with anisotropic dispersion. It should be noted that the modelling of ALOS has given rise to a number of controversies linked in particular to the nature of the gap. Consequently, our study in the one-dimensional case should enable us to estimate the ALOS and to assess whether it is likely to be involved in our case.

The paper is organised as follows: section 2 gives a theoretical approach to calculate the emission spectrum in the band-gap region of a 1D-PC; in section 3, a method is presented to estimate the ALOS in a 1D-PC; finally, the particular case of the Si $L_{2,3}$ emission band from a periodic multilayered structure, made up with 50 Mo/Si bilayers, is considered.

2. Spontaneous emission in a 1D-PC : power spectrum

The system (atom *plus* electromagnetic (EM) reservoir within the PC) is initially in a state $|I\rangle$, where the atom is excited (state $|e\rangle$) without photon in the EM field ; this state is denoted by $|I\rangle = |e, 0\rangle$. The final state of this system is given by $|F_\lambda\rangle = |g, 1_\lambda\rangle$, where the atom is in the ground state $|g\rangle$ and the EM field in the state $|1_\lambda\rangle$ with one photon in the field mode λ . The index λ labels the energy band n in the PC and the wave vector \mathbf{k} of a given mode : $\lambda = |n, \mathbf{k}\rangle$. In the weak coupling regime, the perturbative theory of the SE provides the SE rate through the Fermi golden rule (Zhang and Liu, 2016) :

$$\tau(\omega_0) = \frac{2\pi}{\hbar^2} \rho(\omega_0) |\langle I | \mathbf{H}_{int} | F_\lambda \rangle|^2 \delta(\omega_0 - \omega_k) \quad [1]$$

with \hbar the Planck constant, ω_k the radiation frequency and ω_0 the Bohr frequency of the transition $|e\rangle \rightarrow |g\rangle$.

The interaction Hamiltonian \mathbf{H}_{int} is given in the dipole and rotating wave approximations by :

$$\mathbf{H}_{int} = -\boldsymbol{\mu}_{eg} \cdot \mathbf{E} \quad [2]$$

where $\boldsymbol{\mu}_{eg}$ is the dipole moment of the transition $|e\rangle \rightarrow |g\rangle$ and \mathbf{E} the electric field. In a classical approach, the atomic transition $|e\rangle \rightarrow |g\rangle$ is modelled by a dipole oscillating with frequency ω_0 and with a moment $\boldsymbol{\mu}_{eg}$: the expectation of the quantum dipole $\langle g | q \mathbf{r} | e \rangle$, q and \mathbf{r} being the electron charge and the charge displacement respectively, can be identified with the time-averaged dipole moment of a classical oscillator. Then the steady state (after all transients have vanished) of the power output $P_{\omega_0}(\mathbf{R})$ for a dipole located at \mathbf{R} within the PC reads :

$$P_{\omega_0}(\mathbf{R}) \propto \frac{\pi^2}{2} \omega_0^2 |\boldsymbol{\mu}_{eg}|^2 \int |\mathbf{a}_k(\mathbf{R}, \omega_k)|^2 \delta(\omega_0 - \omega_k) dk \quad [3]$$

where \mathbf{a}_k are the normal modes NMs, k the effective wavenumber of radiation within the PC structure. The NMs are the solutions of the homogeneous Helmholtz equation :

$$\nabla \wedge \nabla \wedge \mathbf{a}_k(\mathbf{R}, \omega_k) - \left(\frac{\omega_k}{c}\right)^2 \varepsilon(\mathbf{R}, \omega_k) \mathbf{a}_k(\mathbf{R}, \omega_k) = \mathbf{0} \quad [4]$$

with the transverse gauge condition :

$$\nabla \cdot (\varepsilon(\mathbf{R}, \omega_k) \mathbf{a}_k(\mathbf{R}, \omega_k)) = 0$$

[5]

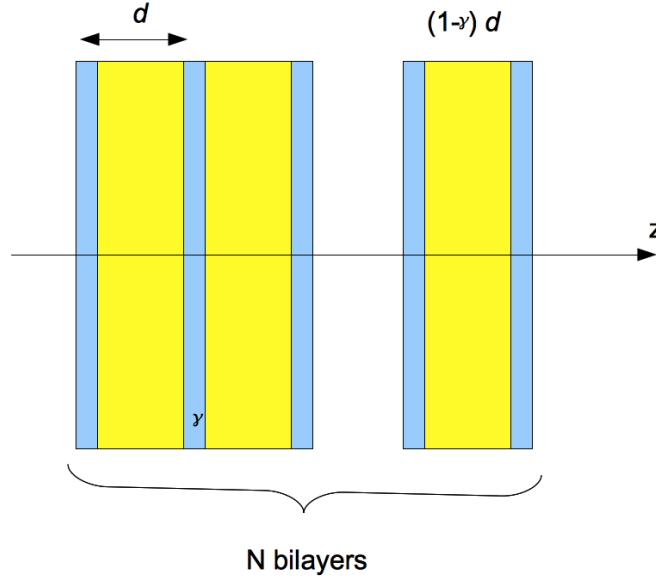


Figure 1 : Sketch of the periodic multilayered structure constituting the PC under consideration in this work. It consists in N bilayers of thickness d ; the thickness of the first layer is γd and the one of the second layer is $(1 - \gamma)d$.

For a periodic multilayered structure made up with N bilayers as shown in figure 1, the NM in the j^{th} layer of the first bilayer ($n = 0$) can be written as the superposition of a propagating and a counter-propagating wave of wave vector normal component $k_{\perp j}, j=1,2$ that is :

$$\mathbf{a}_k(\mathbf{R}, \omega_k) \rightarrow a_j^{(n=0)}(z) = A_j^+ e^{ik_{\perp j}z} + A_j^- e^{-ik_{\perp j}z}$$

[6]

Taking into account the one-dimensional character of the PC, the 3D-variable \mathbf{R} is replaced by the 1D-variable z . By virtue of the Bloch-Floquet theorem, the NM in the $n = p$ bilayer can be generated from the one in $n = 0$:

$$a_j^{(n=p)}(z) = e^{iKpd} (A_j^+ e^{ik_{\perp j}(z-pd)} + A_j^- e^{-ik_{\perp j}(z-pd)}), pd < z < (p+1)d$$

[7]

the quantity K being the Bloch wavenumber corresponding to an infinite structure ($N \rightarrow \infty$).

By applying the continuity conditions of the NMs and its first derivative with respect to the position variable z , it follows that the four coefficients $A_j^\pm, j = 1, 2$ obey the following equation :

$$\hat{C}(k_j, K, d, \gamma) \begin{pmatrix} A_1^+ \\ A_1^- \\ A_2^+ \\ A_2^- \end{pmatrix} = \begin{pmatrix} 0 \\ 0 \\ 0 \\ 0 \end{pmatrix} \quad [8]$$

where \hat{C} is a 4×4 matrix given by :

$$\hat{C}(k_j, K, d, \gamma) = \begin{pmatrix} \exp(i \Gamma_1^+ d) & \exp(i \Gamma_1^- d) & -1 & -1 \\ i k_{\perp 1} \exp(i \Gamma_1^+ d) & -i k_{\perp 1} \exp(i \Gamma_1^- d) & -i k_{\perp 2} & i k_{\perp 2} \\ -\exp(i k_{\perp 1} \gamma d) & -\exp(-i k_{\perp 1} \gamma d) & \exp(i k_{\perp 2} \gamma d) & \exp(-i k_{\perp 2} \gamma d) \\ -i k_{\perp 1} \exp(i k_{\perp 1} \gamma d) & i k_{\perp 1} \exp(-i k_{\perp 1} \gamma d) & i k_{\perp 2} \exp(i k_{\perp 2} \gamma d) & -i k_{\perp 2} \exp(-i k_{\perp 2} \gamma d) \end{pmatrix} \quad [9]$$

with $\Gamma_j^\pm = K \pm k_{\perp j}$.

The condition to obtain non-trivial solutions of [8] is :

$$\text{Det}[\hat{C}(k_j, K, d, \gamma)] = 0 \quad [10]$$

which forms a dispersion equation providing the value of K . To get the full expression of the NM in each layer, one needs the coefficients $A_j^\pm, j = 1, 2$. This can be done by calculating the kernel of $\hat{C}(k_j, K, d, \gamma)$ and imposing the following normalization condition :

$$\int a_j^{(n=p)}(z) a_j^{*(n=p)}(z) dz = \delta_D(k - k') \quad [11]$$

For non-absorbing materials, when the dispersion relationship doesn't have a real solution, that is when K becomes a complex number, then the electromagnetic wave undergoes a regime of forbidden propagation (band gap) with $A_j^\pm = 0$. For absorbing materials, the NM are evanescent waves.

By integrating over k , the density of modes $\rho = \frac{dk}{d\omega_k}$ appears as the result of changing variables k to ω_k , so that the power spectrum of the radiation emitted by the dipole located at \mathbf{R} can be written in the following form :

$$P_{\omega_0}(\mathbf{R}) = S(\omega_0) \rho(\omega_0) |\mathbf{a}_k(\mathbf{R}, \omega_0)|^2 \quad [12]$$

$S(\omega_0)$ is a quantity proportionnal to the SE emission intensity of the bulk material at the frequency ω_0 ; it includes the square of the dipole moment module $|\boldsymbol{\mu}_{eg}|^2$ and the density of electronic states at the atomic level corresponding to the $|e\rangle \rightarrow |g\rangle$ transition of frequency ω_0 .

The total power spectrum P_{ω_0} resulting from the distribution of the dipoles within the PC is obtained by the integration along the PC :

$$P_{\omega_0} = S(\omega_0) \rho(\omega_0) \frac{1}{z_{max} - z_{min}} \int_{z_{min}}^{z_{max}} |\mathbf{a}_k(z, \omega_0)|^2 dz \quad [13]$$

It appears that the DOM $\rho(\omega_0)$ considerably influences the quantity P_{ω_0} . In the free space, the DOM behaves as ω^{-2} while inside the band gap of a PC, it tends to vanish. At the band edges of frequencies ω_d, ω_u , the DOM in a 1D-PC behaves as $1/\sqrt{|\omega_{d,u} - \omega|}$ in the “effective-mass” approximation of the dispersion relation, which means a divergent behavior at the band edge frequencies. In reality, the DOM does not present a sharp shape at the band-edges especially in the soft-x-ray domain but a more or less pronounced peak. The DOM of a 1D-PC can be calculated by means of a formula proposed by Bendickson *et al.* (Bendickson et al., 1996). The DOM $\rho(\omega)$ is given from the real part x and the imaginary part y of the transmission coefficient of the PC as follows :

$$\rho(\omega) = \frac{1}{Nd} \frac{y'x - x'y}{x^2 + y^2} \quad [14]$$

where the prime ‘ denotes differentiation with respect to the radiation frequency. The transmission coefficient can be calculated by means of different approaches, in particular the transfer matrix method (Yeh, 2005; Pardo et al., 1988).

3. Spontaneous emission in a 1D-PC : anomalous Lamb optical shift

The spectral shift or ALOS, that is the difference between the energy level in the dressed atom embedded in the PC and the bare atom in vacuum is approximately given by (see Appendix 1) :

$$\Delta(\omega_0) = \alpha PV \int_{-\infty}^{\infty} \frac{\Omega \rho(\Omega)}{\omega_0 - \Omega} d\Omega, \alpha = \frac{(\mu_{eg})^2}{12 \pi^2 \hbar \varepsilon_0}; \omega_0 = \omega_e - \omega_g \quad [15]$$

It has been pointed out that this radiative correction could come mainly from real photons than virtual photons, in contrast to the vacuum case (Wang et al., 2004).

The shift $\Delta(\omega_0)$ as formulated by Eq. [15] can be rewritten after some algebraic manipulation taking into account that the integrand presents a resonance behavior at the frequency ω_0 , in the following form :

$$\Delta(\omega_0) = \beta \left[PV \int_{-\infty}^{+\infty} \frac{\omega_0 \gamma(\Omega)}{\omega_0 - \Omega} d\Omega - PV \int_{-\infty}^{+\infty} \gamma(\Omega) d\Omega \right] \quad [16]$$

with $\beta = \omega_0^2 \alpha$ and $\gamma(\Omega) = \frac{\rho(\Omega) \Theta(\Omega)}{\Omega^2}$ where the Heaviside function $\Theta(x)$ has been introduced to make explicit that $\gamma(\Omega)$ is only defined for positive frequencies. The second term in the right-hand side of Eq. [16] is linearly divergent and can be removed by an appropriate mass renormalization in the Hamiltonian taking into account that the bare electronic mass is also dressed by the EM field. The first term is at most only logarithmically divergent and to treat (overcome) this divergence, one introduces a cut-off frequency Λ that, following Bethe's method (Bethe, 1947), is taken to be the electron's Compton frequency Λ_c .

Finally, one obtains an approximate expression of the anomalous Lamb shift, in the form :

$$\Delta(\omega_0) = \pi \beta \omega_0 H_{\omega_0}[\gamma(\Omega).Rect(0, \Lambda_c)] \quad [17]$$

where $Rect(x)$ is the rectangle function.

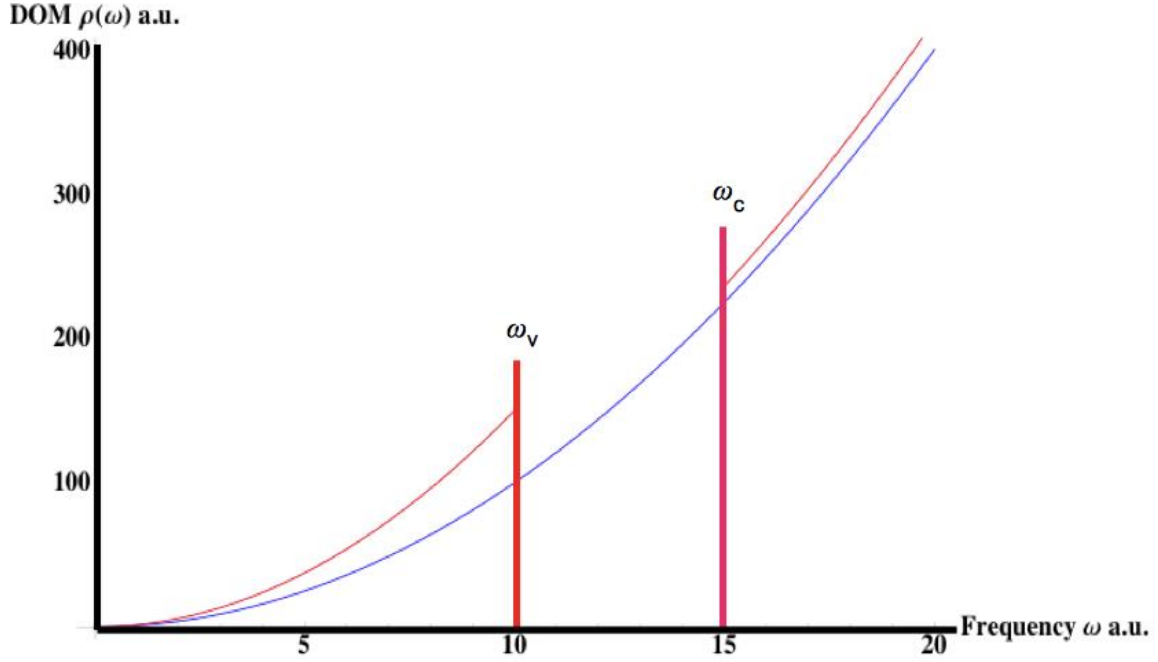


Figure 2 : Typical density of optical modes as a function of radiation frequency ω in a 1D-PC ; the band gap is between ω_v and ω_c ; the blue line shows the DOM variation for a bulk (homogeneous) medium and the red line in a 1D-PC ; peaks shown schematically by red bars may occur at the band edges.

The DOM $\rho(\omega)$ in the 1D-PC can be modelled as follows (see Fig. 2) :

- within the gap that is between ω_v and ω_c , $\rho(\omega)$ is nearly constant and closed to zero ;
- far outside the gap, $\rho(\omega)$ can be taken equal to be the free (vacuum) value that is $\frac{\Omega^2}{c^3}$;
- at the band edges, the DOM may display peaked behaviour corresponding to the singularity of the derivative $\frac{dk}{d\omega}$ appearing in the “effective-mass” approximation for the curve dispersion for a 1D-PC.

Indeed, in the x-ray domain, where absorption plays an important role, the shape of the peaks is rather smooth and can be described at first intention by means of a Lorentzian curve $\rho_{BE}(\Omega) = \rho_{\max BE} \mathcal{L}(\Omega)$ where :

$$\mathcal{L}(\Omega) = \frac{a^2}{(\Omega - \Omega_0)^2 + a^2}$$

[18]

is the Lorentzian function normalized to unity, Ω_0 is the frequency center and $2a$ the FWHM of $\mathcal{L}(\Omega)$ respectively. The quantity $\rho_{\max BE}$ is the maximum of the Lorentzian distribution.

Using this model, $\Delta(\omega_0)$ can be written as :

$$\Delta(\omega_0) = \pi \beta \omega_0 \{ H_{\omega_0} [\gamma_{vac}(\Omega). Rect(0, \omega_v)] + H_{\omega_0} [\gamma_{vac}(\Omega). Rect(\omega_c, \Lambda_c)] + H_{\omega_0} [\gamma_{BE}(\Omega)] \} \quad [19]$$

with $\gamma_{vac}(\Omega) = \frac{1}{\Omega^2} \frac{\Omega^2}{c^3} = \frac{1}{c^3}$; moreover :

$$\gamma_{BE}(\Omega) = \frac{\rho_{\max BE} \mathcal{L}(\Omega) \Theta(\Omega)}{\Omega^2} \quad [20]$$

Applying the following relationship :

$$H[Rect(0, \Lambda)] = \frac{1}{\pi} \int_0^\Lambda \frac{dx}{\omega_0 - x} = -\frac{1}{\pi} \int_0^\Lambda \frac{dx}{x - \omega_0} = -\frac{1}{\pi} [Ln|x - \omega_0|]_0^\Lambda = \frac{1}{\pi} Ln \left| \frac{\omega_0}{\Lambda - \omega_0} \right| \quad [21]$$

it comes :

$$H_{\omega_0} [\gamma_{vac}(\Omega). Rect(0, \omega_v)] = \frac{1}{c^3} H_{\omega_0} [Rect(0, \omega_v)] = \frac{1}{c^3} \frac{1}{\pi} Ln \left| \frac{\omega_0}{\omega_v - \omega_0} \right| \quad [22]$$

and :

$$\begin{aligned} H_{\omega_0} [\gamma_{vac}(\Omega). Rect(\omega_c, \Lambda_c)] &= H_{\omega_0} [\gamma_{vac}(\Omega). Rect(0, \Lambda_c)] - H_{\omega_0} [\gamma_{vac}(\Omega). Rect(0, \omega_c)] \\ &= \frac{1}{c^3} \frac{1}{\pi} \left(Ln \left| \frac{\omega_0}{\Lambda_c - \omega_0} \right| - Ln \left| \frac{\omega_0}{\omega_c - \omega_0} \right| \right) \end{aligned} \quad [23]$$

so that :

$$\Delta(\omega_0) = \frac{\beta \omega_0}{c^3} Ln \left| \frac{\omega_0}{\omega_v - \omega_0} \frac{\omega_c - \omega_0}{\Lambda_c - \omega_0} \right| + \pi \beta \omega_0 H_{\omega_0} [\gamma_{BE}(\Omega)] \quad [24]$$

$$\Delta(\omega_0) = \Delta_G(\omega_0) + \Delta_{BE}(\omega_0)$$

with $\Delta_G(\omega_0)$ the contribution of the gap given by :

$$\Delta_G(\omega_0) = \frac{\beta \omega_0}{c^3} Ln \left| \frac{\omega_0}{\omega_v - \omega_0} \frac{\omega_c - \omega_0}{\Lambda_c - \omega_0} \right| \quad [25]$$

and with $\Delta_{BE}(\omega_0)$ the contribution of the band edges given by :

$$\Delta_{BE}(\omega_0) = \pi \beta \omega_0 H_{\omega_0}[\gamma_{BE}(\Omega)] \quad [26]$$

One can check in absence of gap that $\omega_v = \omega_c$ and $H[\gamma_{BE}(\Omega)] = 0$ and consequently since $\Lambda_c \gg \omega_0$:

$$\Delta(\omega_0) = \frac{\beta \omega_0}{c^3} \text{Ln} \left| \frac{\omega_0}{\Lambda_c - \omega_0} \right| \approx \frac{\beta \omega_0}{c^3} \text{Ln} \left| \frac{\omega_0}{\Lambda_c} \right| \quad [27]$$

which is the usual Wigner-Weisskopf result for the free Lamb shift (in vacuum). The last term denoted $\Delta_{BE}(\omega_0)$ in the right-hand side of Eq. [24] has to be introduced only if the DOM presents peaks at the band edges of the gap. This requires a special treatment. From Eqs. [15,19], it follows that :

$$\Delta_{BE}(\omega_0) = \alpha \text{PV} \int_{-\infty}^{\infty} \frac{\Omega}{\omega_0 - \Omega} \rho_{\max BE} \mathcal{L}(\Omega) d\Omega \quad [27]$$

that is, taking into account Eq. [18] :

$$\Delta_{BE}(\omega_0) = \alpha \rho_{\max BE} \text{PV} \int_{-\infty}^{\infty} \frac{\Omega}{\omega_0 - \Omega} \frac{a^2}{(\Omega - \Omega_0)^2 + a^2} d\Omega \quad [28]$$

The PV integral in Eq. [28] can be rewritten as \wp by doing $t = \Omega - \Omega_0$:

$$\wp = \text{PV} \int_{-\infty}^{\infty} \frac{t + \Omega_0}{\widetilde{\omega}_0 - t} \frac{a^2}{t^2 + a^2} dt ; \widetilde{\omega}_0 = \omega_0 - \Omega_0 \quad [29]$$

or in terms of Hilbert transforms :

$$\wp = \pi a \left\{ \Omega_0 H_{\widetilde{\omega}_0} \left[\frac{a}{t^2 + a^2} \right] + H_{\widetilde{\omega}_0} \left[\frac{t a}{t^2 + a^2} \right] \right\} \quad [30]$$

Using that the fact $\frac{a}{t^2+a^2}$ and $\frac{t a}{t^2+a^2}$ form a pair of Hilbert transformations (Poularikas, 1998), it comes :

$$\wp = \pi a \left\{ \frac{\widetilde{\omega}_0 \Omega_0}{\widetilde{\omega}_0^2 + a^2} - \frac{a}{\widetilde{\omega}_0^2 + a^2} \right\} \quad [31]$$

Finally :

$$\Delta_{BE}(\omega_0) = \alpha \wp = \alpha \rho_{\max BE} \pi a \frac{\widetilde{\omega}_0 \Omega_0 - a}{\widetilde{\omega}_0^2 + a^2}$$

[32]

It appears that $\Delta_{BE}(\omega_0)$ presents a resonant behavior for $\widetilde{\omega}_0 = 0$ that is for $\omega_0 = \Omega_0$. At the resonance :

$$\Delta_{BE}(\omega_0) = -\alpha \rho_{\max BE} \pi a$$

[33]

4. Application to the Si L_{2,3} emission band

To illustrate the above theoretical considerations, we consider the particular case of the Si L_{2,3} emission :

- in a first step, this band emitted from a silicon substrate is recorded by means of a reflection zone plate spectrometer (Hassebi et al., 2024) set up in an CAMECA SX100 electron probe microanalyser ; the detection angle of the emitted radiation is at an angle of 40° with respect to the sample surface ;
- in a second step, we calculate the spectrum of the same emission band from the Si layers embedded in a Mo/Si periodic multilayered structure ; this structure can be regarded as a 1D-PC acting as a Bragg resonator for the Si L_{2,3} emission. Its characteristics are : $N = 50$, $d = 9.76$ nm, $\gamma = 0.2$; it means that the thickness of the Si layer is 1.95 nm while the one of Mo is 7.81 nm and the Bragg resonance takes place at an angle of 47° with respect to the stratification plane.

The choice of this emission and of the PC structure is mainly motivated by the fact that the first order bandgap of the PC is, spectrally speaking, centered on the emission band and covers a large part of the emission band.

Spectrum

The experimental Si L_{2,3} band is sketched on figure 3 in comparison with the theoretical spectrum calculated by means of WIEN2k code (Blaha et al., 2020) implementing the full-potential augmented plane wave method. The generalized gradient approximation of Perdew-Burke-Ernzerhof (Perdew et al., 1996) was used to approximate the exchange-correlation function. The emission spectrum is calculated for the dipole allowed transitions ($\Delta l = \pm 1$), generating matrix elements, which are multiplied with the partial densities of states. It is then convolved by a 0.05 eV wide Lorentzian to account for the lifetime of the core hole (Campbell and Papp, 2001) and by a 0.5 eV wide Gaussian for the instrumental broadening. To align both spectra, the

binding energy of the Si $2p_{3/2}$ core level is fixed at 95.0 eV. There is a good agreement between the measured and simulated spectra. The energy distribution of the emitted photons mainly reflects the energy distribution of the s and d occupied valence states.

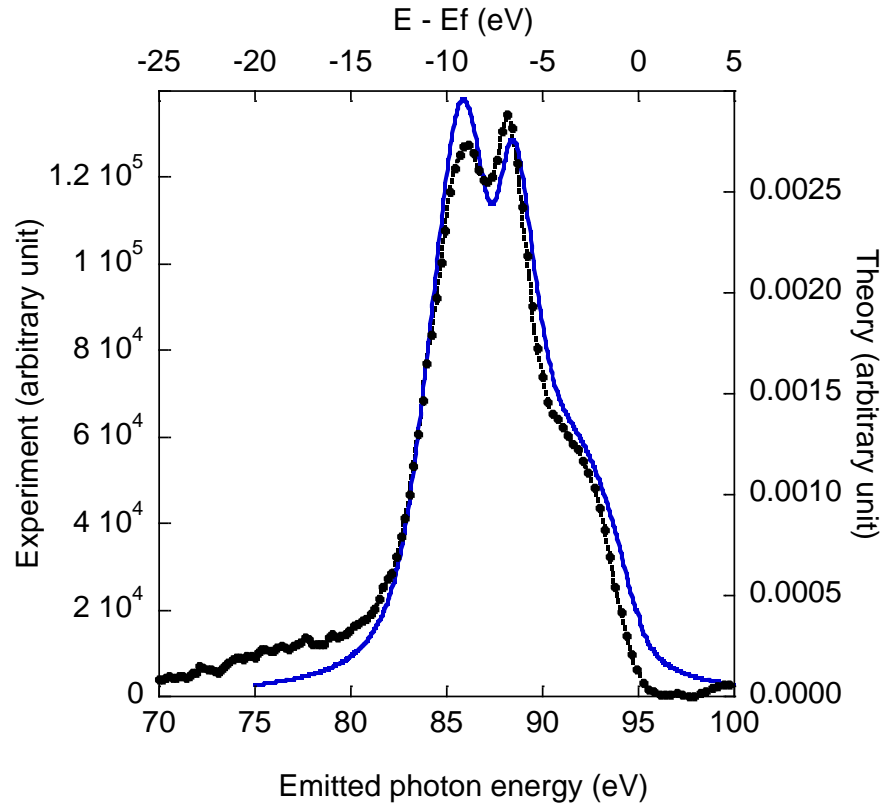


Figure 3 : For a bulk Si sample, experimental (black dotted line) and theoretical (blue line) Si $L_{2,3}$ band as a function of the emitted photon energy and of the binding energy relative to the Fermi level.

Figure 4 presents the calculated Si $L_{2,3}$ band emitted from the PC under consideration using Eq. [13]. The DOM of the PC calculated by means of Eq. [14] is also plotted as a function of the photon energy. To illustrate the characteristics of this PC as Bragg diffracting structure, transmission (Fig. 4-up) is also given. It appears that the PC considerably modifies the spectrum of the Si $L_{2,3}$ band : the fingerprint of the DOM and of the NMs is particularly important within the bandgap where SE is rather totally extinguished. Exaltation of the SE is evidenced at the band-edges while inhibition is observed within the gap, in agreement with the Purcell effect.

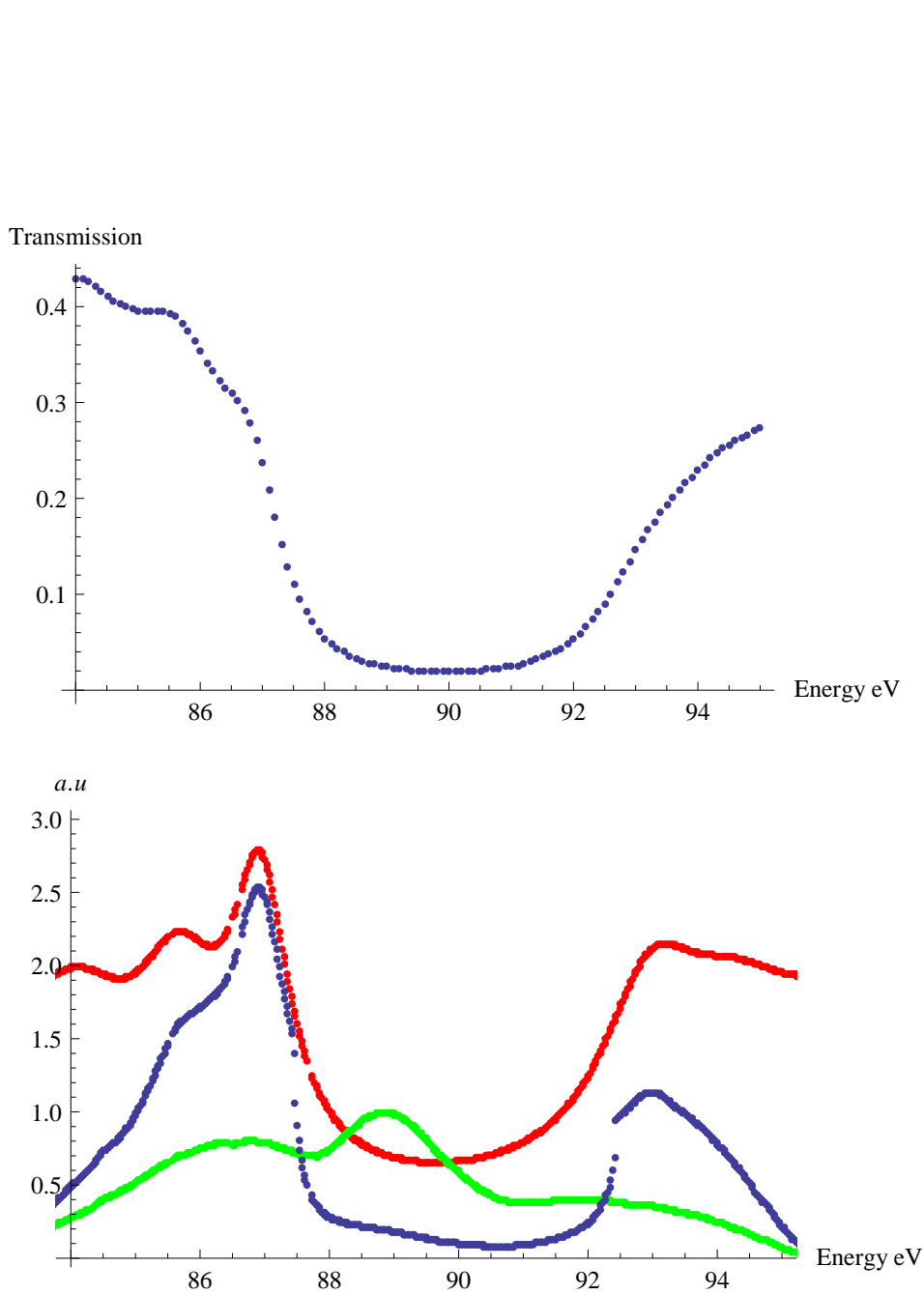


Figure 4 : (down) calculated Si $L_{2,3}$ band emitted from the PC under consideration (blue curve)-see text-, calculated DOM (red curve), experimental Si $L_{2,3}$ band (green curve) band for bulk silicon ; (up) transmission of the PC.

ALOS

From the theoretical approach of section 3, it is possible to estimate the ALOS affecting the Si $L_{2,3}$ band emitted from the PC under consideration. The contribution to the ALOS of the gap, that is $\Delta_G(\omega_0)$ given in Eq. [25], remains practically constant within the gap, but diverges at the band edges at the frequencies ω_v and ω_c ; it approximately

amounts from 3×10^9 to $4 \times 10^9 \text{ s}^{-1}$ in the spectral range covered by the Si $L_{2,3}$ band, which spreads between 85 and 95 eV. This ALOS value is obtained by means of the dipole matrix elements calculated by means of Wien2k code.

The contribution of the band edge at ω_v , that is $\Delta_{BE}(\omega_v)$, is accounted for by a Lorentzian shape of the DOM, see Eq. [18], with $\hbar \Omega_0 = \hbar \omega_v = 87 \text{ eV}$ and $\hbar a = 2 \text{ eV}$; the resonant contribution $\Delta_{BE}(\Omega_0) = -\alpha a \rho_{\max BE} \pi$, see Eq. [33]. The value of $\rho_{\max BE}$ is estimated from the peak value of the DOM at 87 eV (see Fig. 4-down). It follows that $\Delta_{BE}(\Omega_0)$ amounts to approximately $0.3 \times 10^7 \text{ s}^{-1}$ and the relative spectral shift $\Delta_{BE}(\omega_0)/\omega_0$ coming from the anomalous Lamb optical effect is in the order of $10^9/10^{16} = 10^{-7}$.

5. Conclusion

The considered theoretical approach allows us to predict that the Purcell effect must have a strong impact on the spontaneous emission spectrum when the emitted radiation is in Bragg resonance with the photonic crystal, or in other words, if the emission occurs in the region of a band gap. If the emission completely covers the gap in terms of frequency, the part of the SE spectrum inside the gap is strongly inhibited, while those coinciding with the band edges tend to be exalted. In the soft x-ray range, absorption effects attenuate this exaltation compared with that which can occur in the hard x-ray range. The effect of the Lamb shift is relatively small and the resulting shift cannot be observed using a standard spectroscopic method in this spectral range.

Appendix 1 : Anomalous Lamb optical shift ALOS

The dynamical evolution of the system described by the interaction Hamiltonian H_{int} is governed by the time-dependent Schrödinger equation appealing to the evolution operator $U(t)$:

$$i \hbar \frac{dU(t)}{dt} = H_{int} U(t) \quad [A.1]$$

The Hamiltonian H_{int} can be written as the sum of the unperturbed hamiltonian H_0 and of a perturbation potential V : $H_{int} = H_0 + V$. A solution of Eq. [A1] can searched in the form the following expansion :

$$U(t)|I\rangle = b_I(t)|I\rangle + \sum_{\lambda} b_F(t) |g, 1_{\lambda}\rangle \quad [A.2]$$

with the initial conditions :

$$b_I(0) = 1, b_F(0) = 0 \quad [A.3]$$

The problem, that is the determination of the coefficients $b_I(t)$, can be treated by the *resolvante* method using the Green operator $G(z = \omega \pm i \eta) = 1/(z - H_{int})$ called *resolvante* of the Hamiltonian (Reuse, 2007). By means of the *resolvante* $G(z)$, the evolution operator $U(t)$ is given by a contour integral in the complex plane :

$$U(t) = \frac{1}{2\pi i} \oint G(z) \exp(-i t z) dz \quad [A.4]$$

The Green operator $G(z) = 1/(z - H)$ can be expanded in terms of the Green operator $G_0(z) = 1/(z - H_0)$ associated to the unperturbed hamiltonian H_0 and to the potential V :

$$G(z) = G_0(z) + G_0(z) V G_0(z) + G_0(z) V G_0(z) V G_0(z) + \dots \quad [A.5]$$

It follows that a matrix element of $G(z)$ formed on an unperturbed state $|u\rangle$ is given by :

$$\begin{aligned} G_{uu}(z) &\equiv \langle u|G(z)|u\rangle \\ &= \frac{1}{(z - E_u)} \delta_{uu} + \frac{1}{(z - E_u)} V_{uu} \frac{1}{(z - E_u)} \\ &+ \sum_{i \neq 1} \frac{1}{(z - E_u)} V_{ui} \frac{1}{(z - E_i)} V_{iu} \frac{1}{(z - E_u)} + \dots \end{aligned}$$

[A.6]

where E_u, E_i are eigenvalues of H_0 . Introducing the shift operator $R_u(z)$:

$$R_u(z) = V_{uu} + \sum_{l \neq 1} V_{ul} \frac{1}{z - E_l} V_{lu} + \sum_{l \neq 1} \sum_{m \neq 1} V_{ul} \frac{1}{z - E_l} V_{lm} \frac{1}{z - E_m} V_{mu} + \dots$$

[A.7]

It can be shown by using a diagrammatic method (Cohen-Tannoudji et al., 2001) that $G_{uu}(z)$ can be written as :

$$G_{uu}(z) = \frac{1}{(z - E_u)} \sum_{n=0}^{\infty} \left(\frac{R_u(z)}{(z - E_u)} \right)^n$$

[A.8]

that is :

$$G_{uu}(z) = \frac{1}{z - E_u - R_u(z)}$$

[A.9]

If one sets $|u\rangle = |I\rangle = |e, 0\rangle$, using Eq. [A.9], one can obtain $G_{II}(z)$, and then by applying Eq. [A.4] one deduces the probability amplitude $U_{II}(t) = \langle I|U(t)|I\rangle$. To do it, it is convenient to find an approximate formulation of the shift operator allowing obtaining an analytic form of $G_{uu}(z)$. The potential V can be expanded according to the order j of the electron charge q :

$$V = \sum_j V^{(j)}$$

[A.10]

At the second order of this expansion, the shift operator becomes at the approximation of the large wavelengths :

$$\hat{R}_I(E \pm i\eta) = \sum_{\lambda} \frac{|\langle F_{\lambda} | V^{(1)} | I \rangle|^2}{E - E_g \pm i\eta - \hbar \omega}$$

[A.11]

Using the formula : $\frac{1}{x \pm i\eta} = PV \left(\frac{1}{x} \right) \mp i\pi \delta(x)$, where PV stands for the principal value and $\delta(x)$ the Dirac delta function, then it comes :

$$\hat{R}_I(E \pm i\eta) = \hbar [\Delta(E) \mp i\Gamma(E)/2]$$

[A.12]

where :

$$\Delta(E) = \frac{1}{\hbar} PV \sum_{\lambda} \frac{|\langle F_{\lambda} | V^{(1)} | I \rangle|^2}{E - E_g - \hbar \omega}$$

$$\Gamma(E) = \frac{2\pi}{\hbar} \sum_{\lambda} |\langle F_{\lambda} | V^{(1)} | I \rangle|^2 \delta(E - E_g - \hbar \omega)$$

[A.13]

Assuming that the modes are continuously spaced in frequency, one replaces the discrete summation by an integral :

$$\sum_{\lambda} \rightarrow \frac{\mathcal{V}}{(2\pi)^3} \int d\mathbf{k} = \frac{\mathcal{V}}{(2\pi)^3} \int d\Omega k^2 dk$$

[A.14]

where \mathcal{V} is the volume of the unit cell of the PC and $d\Omega$ the space angle element. It appears that $\Delta(E)$ and $\Gamma(E)$ form a pair of Hilbert transforms :

$$\Delta(E) = H_E[\Gamma(E)], \Gamma(E) = -H_E[\Delta(E)]$$

[A.15]

where H_x stands for the Hilbert transformation operator : $H_x[f(x)] = \frac{1}{\pi} \int_{-\infty}^{+\infty} \frac{f(y)}{x-y} dy$.

Moreover one has:

$$\langle F_{\lambda} | V^{(1)} | I \rangle = -i \sqrt{\frac{\hbar \omega}{2 \varepsilon_0 \mathcal{V}}} \hat{\boldsymbol{\epsilon}} \cdot \widehat{\boldsymbol{\mu}}_{eg}$$

[A.16]

where ε_0 is the vacuum permittivity, $\hat{\boldsymbol{\epsilon}}$ and $\widehat{\boldsymbol{\mu}}_{eg}$ are the unit polarization vector of the EM field and the vector of dipole matrix element associated for the transition $|e\rangle \rightarrow |g\rangle$ respectively. From Eq. [A.13, A.14, A.16], it follows :

$$\Delta(\omega) = \frac{(\hat{\boldsymbol{\epsilon}} \cdot \widehat{\boldsymbol{\mu}}_{eg})^2}{\hbar} \frac{\mathcal{V}}{(2\pi)^3} \frac{1}{2 \varepsilon_0 \mathcal{V}} PV \int_{-\infty}^{+\infty} \frac{\omega'}{\omega - \omega_g - \omega'} k^2 \frac{dk}{d\omega'} d\Omega d\omega'$$

[A.17]

Introducing the local density of modes DOM $\rho(\omega')$ by $k^2 \frac{dk}{d\omega'} = \frac{4\pi}{3} \rho(\omega')$, where the factor $\frac{4\pi}{3}$ arises from the spatial integration and orientational averaging of the dipole $\widehat{\boldsymbol{\mu}}_{eg}$, then it comes :

$$\Delta(\omega) = \frac{(\boldsymbol{\mu}_{eg})^2}{\hbar} \frac{1}{2 \pi^2} \frac{1}{2 \varepsilon_0} \frac{4\pi}{3} PV \int_{-\infty}^{\infty} \frac{\omega' \rho(\omega')}{\omega - \omega_g - \omega'} d\omega'$$

[A.18]

References

- André, J.-M., Jonnard, P., 2010. X-ray spontaneous emission control by 1-dimensional photonic bandgap structure. *Eur. Phys. J. D* 57, 411–418.
<https://doi.org/10.1140/epjd/e2010-00050-7>
- Attwood, D., 1999. *Soft X-Rays and Extreme Ultraviolet Radiation: Principles and Applications*. Cambridge University Press.
- Bendickson, J.M., Dowling, J.P., Scalora, M., 1996. Analytic expressions for the electromagnetic mode density in finite, one-dimensional, photonic band-gap structures. *Phys. Rev. E* 53, 4107–4121.
<https://doi.org/10.1103/PhysRevE.53.4107>
- Bethe, H.A., 1947. The Electromagnetic Shift of Energy Levels. *Phys. Rev.* 72, 339–341.
<https://doi.org/10.1103/PhysRev.72.339>
- Blaž, P., Schwarz, K., Tran, F., Laskowski, R., Madsen, G.K.H., Marks, L.D., 2020. WIEN2k: An APW+lo program for calculating the properties of solids. *J. Chem. Phys.* 152, 074101. <https://doi.org/10.1063/1.5143061>
- Campbell, J.L., Papp, T., 2001. Widths of the atomic K–N7 levels. *At. Data Nucl. Data Tables* 77, 1–56. <https://doi.org/10.1006/adnd.2000.0848>
- Chauvineau, J.-P., Bridou, F., 1996. Analyse angulaire de la fluorescence du fer dans une multicouche périodique Fe/C. *J. Phys. IV* 06, C7-53-C7-64.
<https://doi.org/10.1051/jp4:1996707>
- Chauvineau, J.-P., Hainaut, O., Bridou, F., 1996. Lignes de Kossel observées avec des multicouches périodiques Fe/C. *J. Phys. IV* 06, C4-773-C4-779.
<https://doi.org/10.1051/jp4:1996475>
- Cohen-Tannoudji, C., Dupont-Roc, J., Grynberg, G., 2001. *Processus d'interaction entre photons et atomes*. EDP Sciences.
- Dowling, J.P., Bowden, C.M., 1992. Atomic emission rates in inhomogeneous media with applications to photonic band structures. *Phys. Rev. A* 46, 612–622.
<https://doi.org/10.1103/PhysRevA.46.612>
- Gog, Th., Novikov, D., Falta, J., Hille, A., Materlik, G., 1994. Kossel diffraction and X-ray standing waves: two birds of one feather. *J. Phys. IV* 04, C9-449-C9-452.
<https://doi.org/10.1051/jp4:1994974>
- Haber, J., Gollwitzer, J., Francoual, S., Tolkiehn, M., Strempler, J., Röhlberger, R., 2019. Spectral Control of an X-Ray L-Edge Transition via a Thin-Film Cavity. *Phys. Rev. Lett.* 122, 123608. <https://doi.org/10.1103/PhysRevLett.122.123608>
- Haroche, S., Kleppner, D., 2008. Cavity Quantum Electrodynamics. *Phys. Today* 42, 24.
<https://doi.org/10.1063/1.881201>
- Hassebi, K., Rividi, N., Fialin, M., Verlaquet, A., Godard, G., Probst, J., Löchel, H., Krist, T., Braig, C., Seifert, C., Benbalagh, R., Vacheresse, R., Ilakovac, V., Guen, K.L., Jonnard, P., 2024. High-resolution x-ray emission spectrometry in the lithium K range with a reflection zone plate spectrometer. *X-Ray Spectrom.* n/a.
<https://doi.org/10.1002/xrs.3427>
- John, S., Quang, T., 1995. Localization of Superradiance near a Photonic Band Gap. *Phys. Rev. Lett.* 74, 3419–3422. <https://doi.org/10.1103/PhysRevLett.74.3419>
- John, S., Quang, T., 1994. Spontaneous emission near the edge of a photonic band gap. *Phys. Rev. A* 50, 1764–1769. <https://doi.org/10.1103/PhysRevA.50.1764>
- John, S., Wang, J., 1991. Quantum optics of localized light in a photonic band gap. *Phys. Rev. B* 43, 12772–12789. <https://doi.org/10.1103/PhysRevB.43.12772>

- John, S., Wang, J., 1990. Quantum electrodynamics near a photonic band gap: Photon bound states and dressed atoms. *Phys. Rev. Lett.* 64, 2418–2421.
<https://doi.org/10.1103/PhysRevLett.64.2418>
- Kuroda, K., Sawada, T., Kuroda, T., Watanabe, K., Sakoda, K., 2009. Doubly enhanced spontaneous emission due to increased photon density of states at photonic band edge frequencies. *Opt. Express* 17, 13168–13177.
<https://doi.org/10.1364/OE.17.013168>
- Lambropoulos, P., Nikolopoulos, G.M., Nielsen, T.R., Bay, S., 2000. Fundamental quantum optics in structured reservoirs. *Rep. Prog. Phys.* 63, 455.
<https://doi.org/10.1088/0034-4885/63/4/201>
- Le Guen, K., André, J.-M., Wu, M., Ilakovac, V., Delmotte, F., de Rossi, S., Bridou, F., Meltchakov, E., Giglia, A., Nannarone, S., Wang, Z., Huang, Q., Zhang, Z., Zhu, J., Tu, Y., Yuan, Y., Vickridge, I., Schmaus, D., Briand, E., Steydli, S., Walter, P., Jonnard, P., 2019. Kossel Effect in Periodic Multilayers. *J. Nanosci. Nanotechnol.* 19, 593–601.
<https://doi.org/10.1166/jnn.2019.16472>
- Liu, Q., Song, H., Wang, W., Bai, X., Wang, Y., Dong, B., Xu, L., Han, W., 2010. Observation of Lamb shift and modified spontaneous emission dynamics in the $\text{YBO}_3:\text{Eu}^{3+}$ inverse opal. *Opt. Lett.* 35, 2898–2900. <https://doi.org/10.1364/OL.35.002898>
- Nabiev, R.F., Yeh, P., Sanchez-Mondragon, J.J., 1993. Dynamics of the spontaneous emission of an atom into the photon-density-of-states gap: Solvable quantum-electrodynamical model. *Phys. Rev. A* 47, 3380–3384.
<https://doi.org/10.1103/PhysRevA.47.3380>
- Pardo, B., Megademi, T., André, J.-M., 1988. X-UV synthetic interference mirrors : theoretical approach. *Rev. Phys. Appliquée* 23, 1579–1597.
<https://doi.org/10.1051/rphysap:0198800230100157900>
- Perdew, J.P., Burke, K., Ernzerhof, M., 1996. Generalized Gradient Approximation Made Simple. *Phys. Rev. Lett.* 77, 3865–3868.
<https://doi.org/10.1103/PhysRevLett.77.3865>
- Poularikas, A.D. (Ed.), 1998. *The Hilbert Transform, in: Handbook of Formulas and Tables for Signal Processing.* CRC Press.
- Purcell, E.M., 1946. Spontaneous emission probabilities at radio frequencies. *Phys. Rev.* 69, 681–681. <https://doi.org/10.1103/PhysRev.69.674.2>
- Reuse, F.A., 2007. *Electrodynamique et optique quantiques.* EPFL Press, Lausanne.
- Sheremet, A.S., Petrov, M.I., Iorsh, I.V., Poshakinskiy, A.V., Poddubny, A.N., 2023. Waveguide quantum electrodynamics: Collective radiance and photon-photon correlations. *Rev. Mod. Phys.* 95, 015002.
<https://doi.org/10.1103/RevModPhys.95.015002>
- Tocci, M.D., Scalora, M., Bloemer, M.J., Dowling, J.P., Bowden, C.M., 1996. Measurement of spontaneous-emission enhancement near the one-dimensional photonic band edge of semiconductor heterostructures. *Phys. Rev. A* 53, 2799–2803.
<https://doi.org/10.1103/PhysRevA.53.2799>
- Vats, N., John, S., Busch, K., 2002. Theory of fluorescence in photonic crystals. *Phys. Rev. A* 65, 043808. <https://doi.org/10.1103/PhysRevA.65.043808>
- Wang, X.-H., Kivshar, Y.S., Gu, B.-Y., 2004. Giant Lamb Shift in Photonic Crystals. *Phys. Rev. Lett.* 93, 073901. <https://doi.org/10.1103/PhysRevLett.93.073901>
- Yablonovitch, E., Gmitter, T.J., 1989. Photonic band structure: The face-centered-cubic case. *Phys. Rev. Lett.* 63, 1950–1953.
<https://doi.org/10.1103/PhysRevLett.63.1950>

- Yablonovitch, E., Gmitter, T.J., Leung, K.M., 1991. Photonic band structure: The face-centered-cubic case employing nonspherical atoms. *Phys. Rev. Lett.* 67, 2295–2298. <https://doi.org/10.1103/PhysRevLett.67.2295>
- Yeh, P., 2005. *Optical Waves in Layered Media*. Wiley.
- Zhang, J.M., Liu, Y., 2016. Fermi's golden rule: its derivation and breakdown by an ideal model. *Eur. J. Phys.* 37, 065406. <https://doi.org/10.1088/0143-0807/37/6/065406>
- Zhu, S.-Y., Chen, H., Huang, H., 1997. Quantum Interference Effects in Spontaneous Emission from an Atom Embedded in a Photonic Band Gap Structure. *Phys. Rev. Lett.* 79, 205–208. <https://doi.org/10.1103/PhysRevLett.79.205>